

Article

Direct Synthesis of Chain-End Toluene Functionalized Hyperbranched Ethylene Oligomers

Jianhai Chen ^{1,†}, Zhengpeng Yan ^{2,3,†}, Zhongyuan Li ⁴ and Shengyu Dai ^{2,3,*} 

¹ Analysis and Testing Center, NERC Biomass of Changzhou University, Changzhou University, Changzhou 213164, China; jhchen@cczu.edu.cn

² School of Chemical and Environmental Engineering, Anhui Polytechnic University, Wuhu 241000, China; yan_zp1998@163.com

³ Institutes of Physical Science and Information Technology, Key Laboratory of Structure and Functional Regulation of Hybrid Materials of Ministry of Education, Anhui University, Hefei 230601, China

⁴ Anhui Laboratory of Molecule-Based Materials, Key Laboratory of Functional Molecular Solids, Ministry of Education, School of Chemistry and Materials Science, Anhui Normal University, Wuhu 241002, China; zhongyuanli@ahnu.edu.cn

* Correspondence: daiyu@ustc.edu.cn; Tel.: +86-13955189794

† These authors contributed equally to this work.

Abstract: Chain-end functionalized polymers play an important role in the field of building complex macromolecular structures. In this study, we have synthesized and characterized four dibenzhydryl iminopyridine Ni(II) complexes bearing remote flexible substituents (Et and n-Bu) to provide hyperbranched ethylene oligomers in ethylene oligomerization with moderate to good activities. Most notably, toluene-end-functionalized hyperbranched ethylene oligomers were obtained under elevated temperature conditions and validated by NMR. The tandem catalysis of ethylene oligomerization and the subsequent Friedel–Crafts addition of the resulting unsaturated products to toluene molecules was proposed as the cause of the observed phenomenon.

Keywords: iminopyridine Ni(II) complexes; ethylene oligomerization; hyperbranched; toluene-end-functionalized



Citation: Chen, J.; Yan, Z.; Li, Z.; Dai, S. Direct Synthesis of Chain-End Toluene Functionalized Hyperbranched Ethylene Oligomers. *Polymers* **2022**, *14*, 3049. <https://doi.org/10.3390/polym14153049>

Academic Editor: Béla Iván

Received: 3 July 2022

Accepted: 25 July 2022

Published: 28 July 2022

Publisher's Note: MDPI stays neutral with regard to jurisdictional claims in published maps and institutional affiliations.



Copyright: © 2022 by the authors. Licensee MDPI, Basel, Switzerland. This article is an open access article distributed under the terms and conditions of the Creative Commons Attribution (CC BY) license (<https://creativecommons.org/licenses/by/4.0/>).

1. Introduction

Chain-end functionalized polymers exhibit significant importance in the field of building complex macromolecular structures [1–3]. There are three main types of methods which have been reported to synthesize chain-end functionalized polymers. The first reported approach is that of living coordination polymerization of monomers, followed by in situ chain end reaction modification [4–7]. It is clear that such a method has inherent drawbacks, where the catalyst can only initiate one polymer chain per catalyst, thus limiting its efficiency and yield significantly. The second approach is the in situ one-pot method of chain-end functionalization by chain transfer [8–16]. Each catalyst is capable of generating a number of polymer chains. Due to the efficiency of this type of approach, it can play an important role in certain situations. For example, some early transition-metal catalysts are widely used in chain transfer chain-end functionalization reactions, which are capable of H-X σ -bond metathesis, such as an amine (H–NR₂), borane (H–BR₂). The final reported approach is chain-end functionalization of polymers by modification of unsaturated end groups of synthesized polymers, which is also a common approach. Though great success has been achieved with this strategy, there are several limitations which need to be overcome, such as difficulty in quantitatively converting terminal unsaturated bonds, due to the low concentration of terminal double bonds in polymers and the harshness of polymer solubility [17].

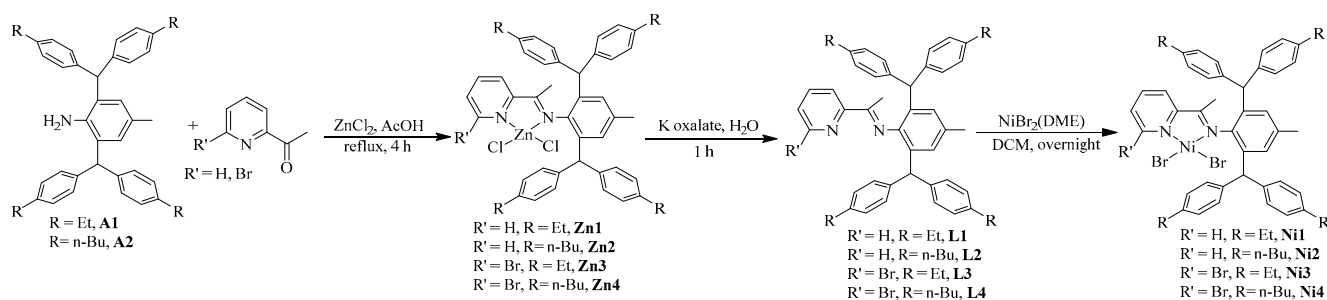
In recent years, an impressive effort has been devoted to exploring late-transition metal-catalyzed ethylene (co)oligomerization, which enables the synthesis of branched and

even hyperbranched ethylene oligomers and co-oligomers [18–25]. Recently, many novel iminopyridine Ni(II) and Pd(II) complexes were designed for ethylene (co)oligomerization due to the unilateral axial steric structure of the iminopyridine ligands, which facilitates the chain transfer reaction during (co)oligomerization [26–35]. In this contribution, a series of rigid–flexible double-layer steric iminopyridine Ni(II) complexes, containing bulky diarylmethyl substituents with remote alkyl moieties, were synthesized and employed for ethylene oligomerization. Surprisingly, chain end toluene functionalized hyperbranched ethylene oligomers were prepared in situ in one pot.

2. Results and Discussions

2.1. Synthesis and Characterization of Iminopyridine Ni(II) Complexes

Dibenzhydryl anilines **A1** and **A2** with remote flexible substituents (Et and n-Bu) were synthesized according to our previous work [30]. The iminopyridine ligands **L1–L4** were obtained from **A1** and **A2** with different 6-substituted 2-acetylpyridine by using the template-type method (Scheme 1) [30]. The ligands were obtained in good yields (60–72%) without chromatography and characterized by NMR (Figures S1–S8) and high-resolution mass spectra (Figures S9–S12). Then, the ligands reacted with 1.0 equiv. of NiBr₂(DME) in dichloromethane at room temperature producing the corresponding Ni(II) complexes **Ni1–Ni4** in 75–85% yields (Scheme 1). The identity and purity of **Ni1–Ni4** were confirmed by MALDI-TOF MS (Figures S13–S16) and elemental analysis. A single crystal of **Ni1** was available from layering its CH₂Cl₂ solution with hexanes at ambient temperature (Figure 1). The complex **Ni1** was crystallized as a centrosymmetric dimer and each Ni(II) atom coordinated with two bridging bromine atoms and one iminopyridine ligand. One terminal bromine atom completed the square-pyramidal coordination sphere of the **Ni1** molecular structure. The dibenzhydryl groups deviated from the catalytic center, which might indicate that the complexes with dibenzhydryl substituents could not maintain an effective shielding on the catalytic center, leading to an easy chain transfer during the oligomerization process.



Scheme 1. Synthesis of iminopyridine ligands and the corresponding nickel complexes.

2.2. Ethylene Oligomerization

With 200 equiv. of Et₂AlCl activated, the complexes **Ni1** and **Ni2** with H at the 6-position of the pyridine ring exhibited high activities (ca. 10⁶ g·mol⁻¹·h⁻¹), whereas the complexes **Ni3** and **Ni4** with Br at the same position performed moderate activities (ca. 10⁵ g·mol⁻¹·h⁻¹) of ethylene oligomerization (Table 1). All of the Ni(II) catalysts yielded low molecular weight (ca. 0.2–3.7 kg/mol) ethylene oligomers with high branching densities (76–94/1000 C) (Table 1). Interestingly, both the catalytic activity and molecular weight decreased as the reaction temperature increased. This was mainly attributed to the elevated temperatures enhancing chain transfer more than chain growth with the nickel catalysts and reducing the solubility of ethylene in toluene. Generally, complexes **Ni1–Ni2** with H at the 6-position of the pyridine ring exhibited higher activities than complexes **Ni3–Ni4** with Br, as well as yielding higher molecular weight ethylene oligomers, which was mainly due to the presence of the Br atom at the 6-position of the pyridine ring hindering the coordination and insertion of ethylene in the oligomerization process [32].

The slowing down of chain growth with little effect on chain transfer directly leads to a decrease of molecular weight. Compared to Ni1 with an ethyl group, Ni2 with a long chain butyl group showed lower activities and produced higher molecular weight ethylene oligomers at 30–70 °C (entries 1–3 vs. 4–6, Table 1). These results indicated that the long chain butyl groups were helpful to improve the molecular weight of the resulting oligomers at the expense of activity. The latter was mainly attributed to the fact that the long chain alkyl substituents with large steric hindrance facilitated the impediment of chain transfer reactions while, in the meantime, discouraging the coordination and insertion of ethylene.

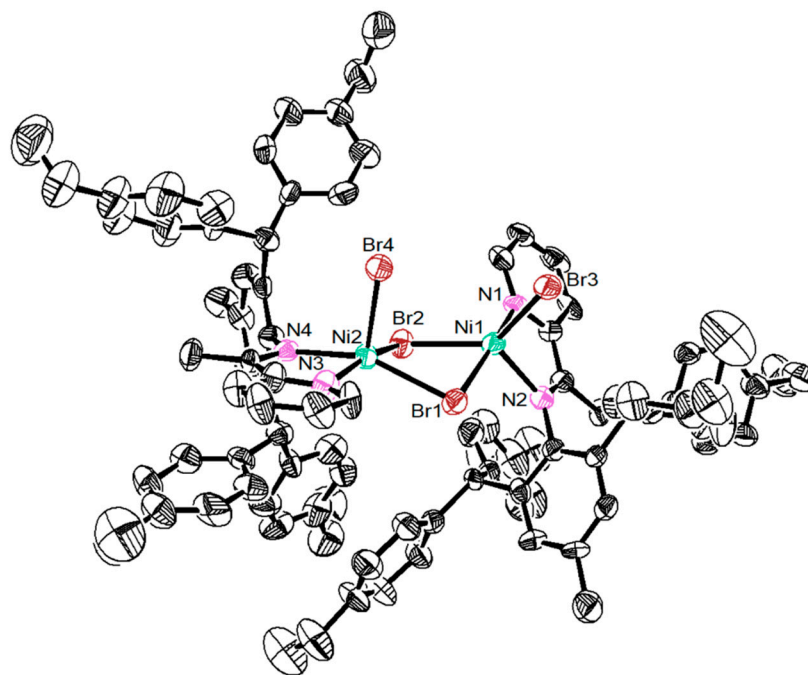


Figure 1. The single crystal structure of nickel complex Ni1 (CCDC: 2080105; 30% probability level), H atoms and solvent molecules have been omitted for clarity.

Table 1. Effect of Catalysts and Temperatures on Ethylene Oligomerization.

Ent.	Precat.	$T/^\circ\text{C}$	Yield/g	Act. ^b	M_n ^c	M_w/M_n ^c	B ^d	F–C ^e
1	Ni1	30	3.54	1.77	3.6	1.42	78	0%
2	Ni1	50	3.10	1.55	3.1	1.38	84	0%
3	Ni1	70	2.98	1.49	2.8	1.28	93	100%
4	Ni2	30	3.02	1.51	3.6	1.45	78	0%
5	Ni2	50	2.81	1.41	3.7	1.37	79	0%
6	Ni2	70	2.31	1.16	3.0	1.31	94	100%
7	Ni3	30	1.00	0.50	1.3	1.04	81	Part
8	Ni3	50	0.65	0.33	0.8	1.04	76	100%
9	Ni3	70	0.47	0.24	0.2 ^f	– ^f	– ^f	100%
10	Ni4	30	0.45	0.23	1.6	1.05	76	Part
11	Ni4	50	0.43	0.22	1.2	1.03	78	100%
12	Ni4	70	0.30	0.15	0.2 ^f	– ^f	– ^f	100%

^a General conditions: complexes (2 μmol), Et_2AlCl (200 equiv.), 1 mL CH_2Cl_2 , 20 mL toluene, time = 1.0 h, ethylene = 6 atm. ^b Activity (Act.) = 10^6 g/(mol Ni·h). ^c Molecular weights (kg mol^{-1}) determined by GPC in THF at 40 °C vs. polystyrene standards. ^d brs = Number of branches per 1000 C, as determined by ^1H NMR spectroscopy. ^e Conversion of the Friedel–Crafts reaction, as determined by ^1H NMR spectroscopy. ^f Molecular weight below the detection limit of GPC, GC-MS detection of molecular weight around 0.2 kg/mol.

NMR spectra were utilized to analyze the microstructure of the produced ethylene oligomers. Interestingly, in the ^1H NMR spectra of the ethylene oligomers formed at 30 and 50 °C in toluene with complexes Ni1 and Ni2 (Table 1, entries 1, 2, 4, and 5), internal olefinic

(major, CH=CH, 5.48–5.30 ppm) or vinylic (minor, CH₂=CH, 5.03 ppm and 4.95 ppm) proton signals were observed as the unsaturated chain end group (Figure 2A). However, the ethylene oligomers obtained at 30 °C in toluene with complexes Ni3–Ni4 showed not only internal olefinic (major, CH=CH, 5.48–5.30 ppm) or vinylic (minor, CH₂=CH, 5.03 ppm and 4.95 ppm) proton signals but also the aromatic proton resonances (6.80–7.22 ppm) (Figure 2B). Further raising the reaction temperature to 50–70 °C with Ni1–Ni2 (70 °C) and Ni3–Ni4 (50 and 70 °C) led to complete disappearance of olefinic proton signals and aromatic proton resonances (6.80–7.22 ppm) were detected exclusively as the chain ends (Figure 2C), which suggested the formation of toluene-end-functionalized branched ethylene oligomers. It implied that the process might undergo a tandem catalysis of ethylene oligomerization and the subsequent Friedel–Crafts addition of the resulting unsaturated ethylene oligomers to solvent molecules (Scheme 2). More importantly, the ratio of toluene-end-functionalized ethylene oligomers could be facily controlled by catalyst structure and reaction temperature. The microstructure of a typical ethylene oligomer (Table 1, entry 2) was verified by the ¹³C NMR analysis (Figure 3) [36–38]. The ¹³C NMR spectrum confirmed the presence of branches of various chain lengths (B1, B2, B3 and Bn branches), olefinic carbons, and sec-butyl structures (Figure 3). Among them, terminal methyl group and methyl branches dominated all the branches, and hyperbranched structures were observed as well, as evidenced by the existence of sec-butyl groups [18]. The chain-end toluene functionalized hyperbranched ethylene oligomers could be used in lubricant and surfactant applications [18].

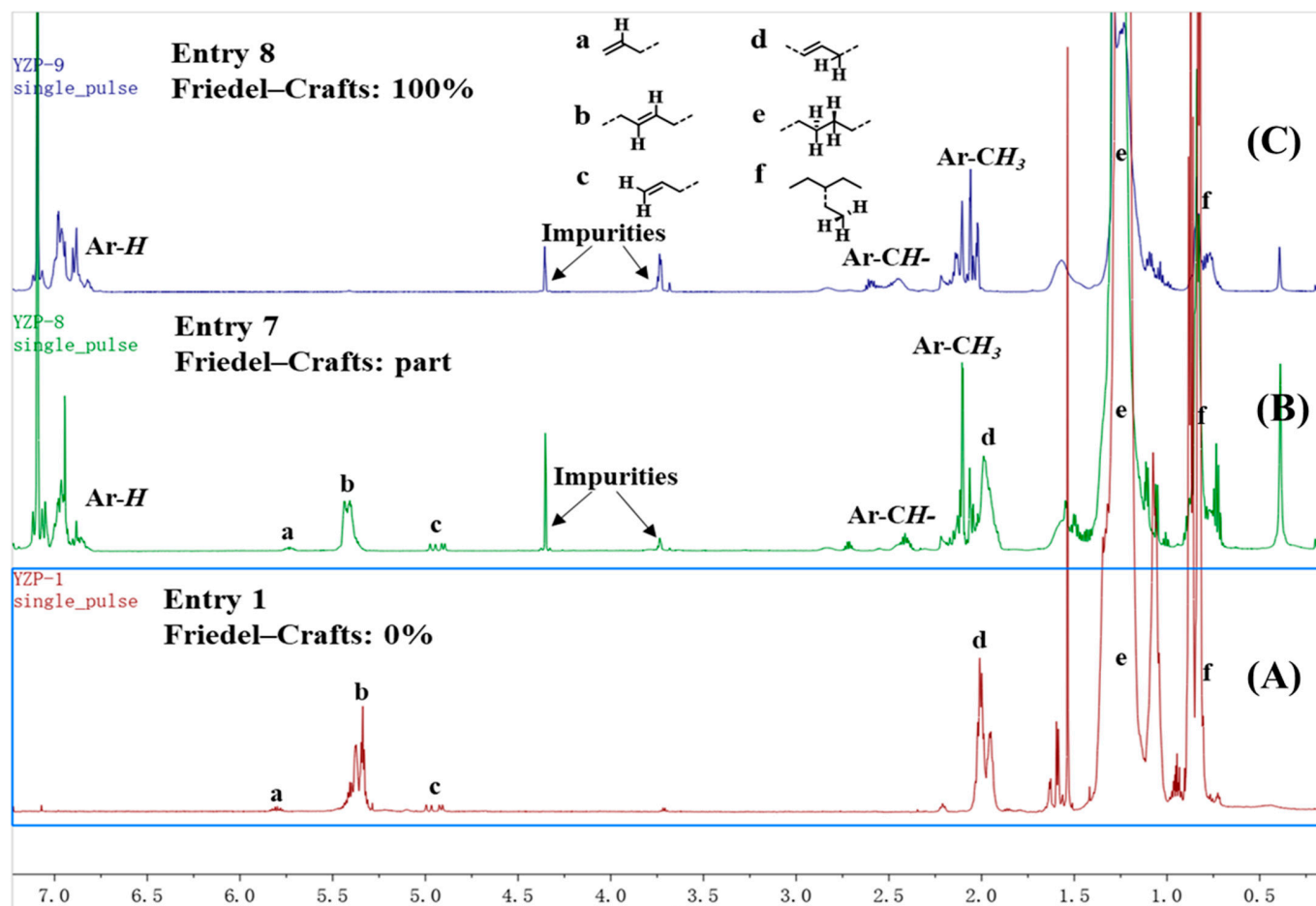
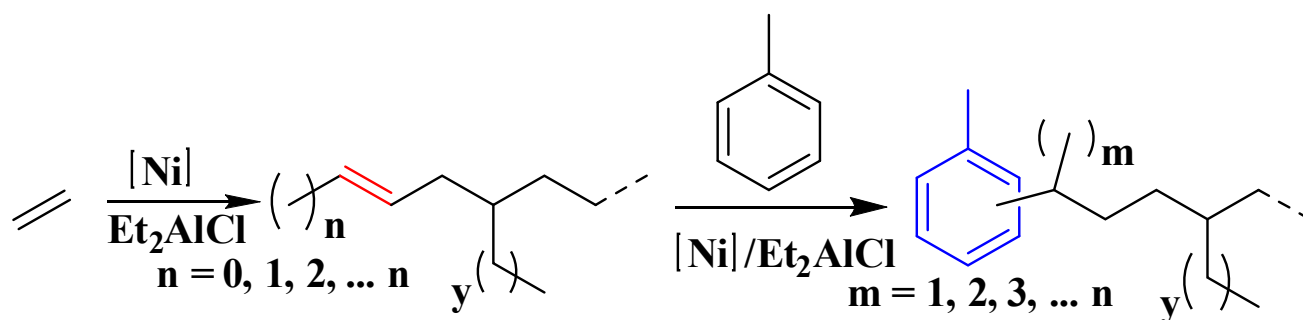


Figure 2. ¹H NMR spectrum (C₆D₆) of representative oligomer samples from Table 1, entries 1 (A), 7 (B) and 8 (C).



Scheme 2. Mechanism of the tandem catalysis of ethylene oligomerization and the subsequent Friedel–Crafts addition to the toluene molecule.

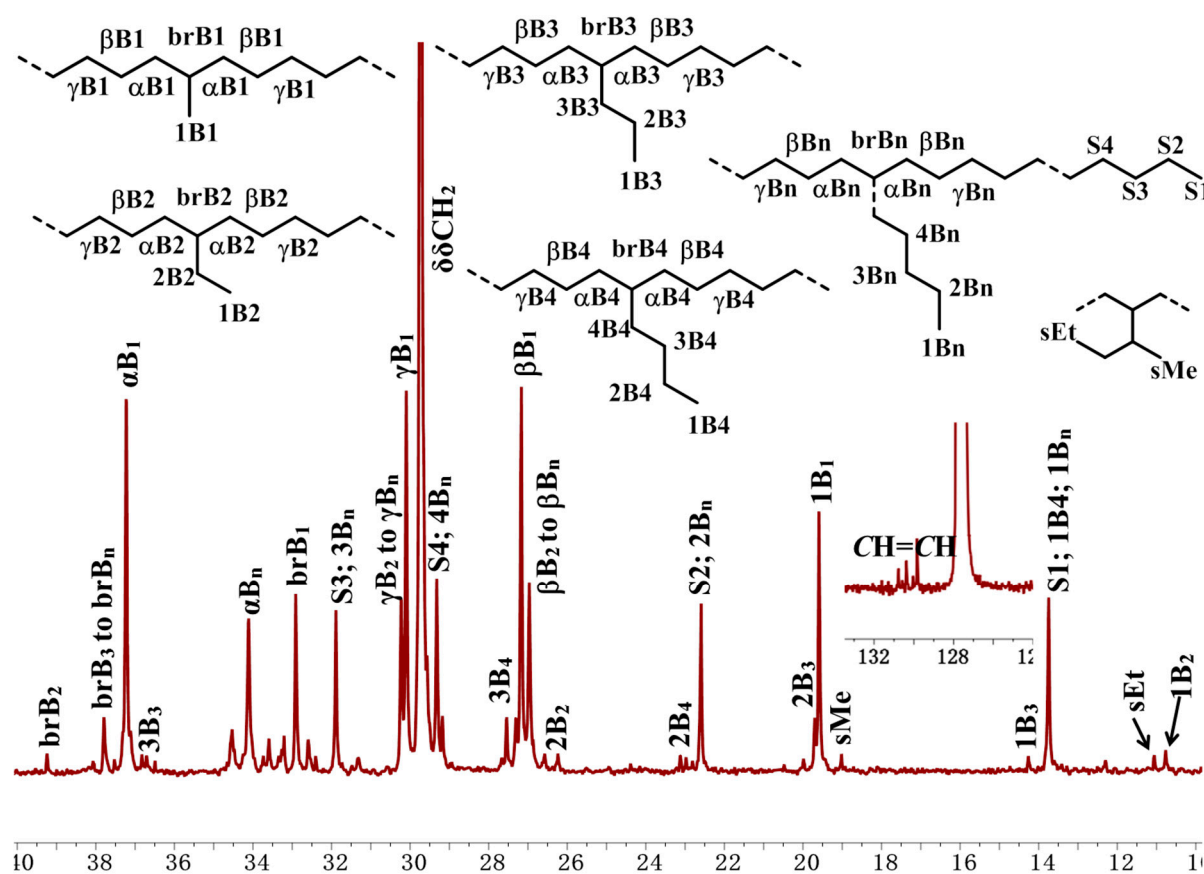


Figure 3. Detailed analysis of ^{13}C NMR spectrum (C_6D_6) of the hyperbranched oligomer sample from entry 2, Table 1. Assignments are labeled by reference [36–38].

3. Conclusions

In summary, we have synthesized and characterized four dibenzhydryl iminopyridine Ni(II) complexes bearing remote flexible substituents (Et and *n*-Bu). Complexes Ni1–Ni2 with H at the 6-position of the pyridine ring performed high activities (ca. $10^6 \text{ g}\cdot\text{mol}^{-1}\cdot\text{h}^{-1}$) while complexes Ni3–Ni4 with Br at the 6-position of the pyridine showed moderate activities (ca. $10^5 \text{ g}\cdot\text{mol}^{-1}\cdot\text{h}^{-1}$) of ethylene oligomerization. Highly branched (76–94/1000 C) ethylene oligomers with various molecular weight sizes were produced in the above catalytic system. Most notably, toluene-end-functionalized hyperbranched ethylene oligomers, validated by NMR, were obtained under elevated temperature conditions. A plausible mechanism was also demonstrated, which underwent tandem catalysis of ethylene oligomerization and the subsequent Friedel–Crafts addition of the resulting unsaturated ethylene oligomers to toluene.

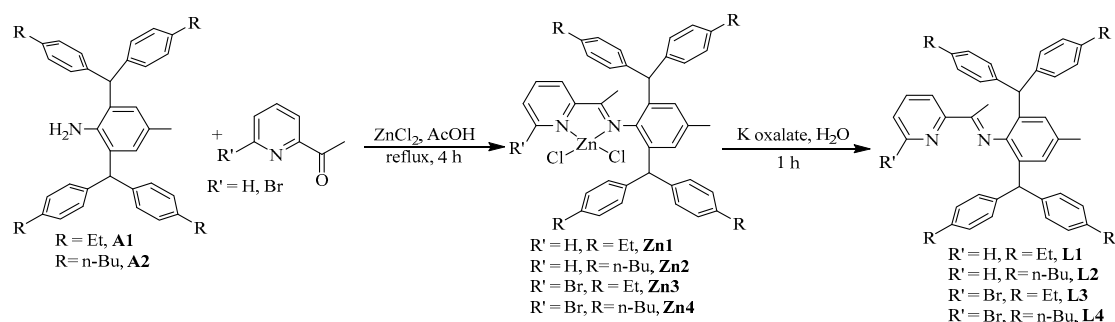
4. Experimental Sections

4.1. General Considerations

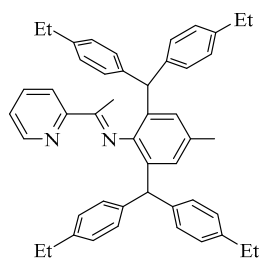
All chemicals were commercially sourced, except those having synthesis as described. All experiments were carried out under a dry nitrogen atmosphere using standard Schlenk techniques or in a glove-box. Deuterated solvents used for NMR were dried and distilled prior to use. The ^1H and ^{13}C NMR spectra were recorded by a JNM-ECZ600R or JNM-ECZ400R spectrometer at ambient temperature unless otherwise stated. The chemical shifts of the ^1H and ^{13}C NMR spectra were referenced to the residual solvent, with coupling constants in Hz. Mass spectra were obtained by the Analytical Center of Anhui University. Elemental analysis was performed by the Analytical Center of Anhui University. X-ray Diffraction data were collected at 293(2) K on a Bruker Smart CCD area detector with graphite-mono-chromated Mo $K\alpha$ radiation ($\lambda = 0.71073 \text{ \AA}$). The molecular weight and the molecular weight distribution of the polymers were determined by gel permeation chromatography (GPC) equipped with two linear Styragel columns (HR2 and HR4) at $40 \text{ }^\circ\text{C}$, using THF as a solvent and calibrated with polystyrene standards. THF was employed as the eluent at a flow rate of 1.0 mL/min .

4.2. Procedure for the Synthesis of Ligands L1–L4

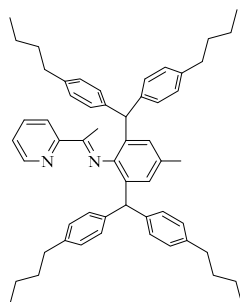
Anilines **A1–A2** were synthesized according to our previous work [30]. The ligands **L1–L4** were prepared as follows: ZnCl_2 (0.34 g, 2.5 mmol) and 2-acetylpyridine (3.0 mmol), were suspended in glacial acetic acid (5 mL). Anilines (2 mmol) were then added, and the reaction mixture was refluxed under stirring for 4 h. The solution was allowed to cool to room temperature, and a bright yellow solid precipitated. The solid was separated by filtration and washed with acetic acid ($3 \times 5 \text{ mL}$) and diethyl ether ($5 \times 5 \text{ mL}$) to remove the remaining acetic acid. Drying under vacuum gave a bright yellow and poorly soluble solid. Then, the zinc was removed from the zinc diimine complex. The product of the previous step was suspended in methylene chloride (30 mL), and a solution of potassium oxalate (0.41 g, 2.2 mmol) in water (5 mL) was added. The reaction mixture was stirred vigorously for 1 h. The two phases were separated, and the organic layer was washed with water ($3 \times 20 \text{ mL}$) and dried with MgSO_4 . After filtration, the solvent was removed under vacuum to obtain the product as a yellow powder and dried under high vacuum. The ligands **L1–L2** were also known [30].



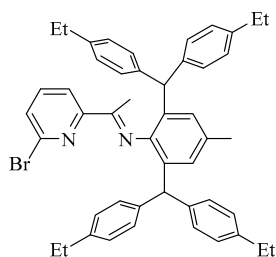
L1 (0.92 g, 70%). ^1H NMR (600 MHz, CDCl_3) δ 8.61 (d, $J = 3.9 \text{ Hz}$, 1H, Ar-H), 8.10 (d, $J = 8.1 \text{ Hz}$, 1H, Ar-H), 7.80–7.66 (m, 1H, Ar-H), 7.42–7.30 (m, 1H, Ar-H), 7.08 (d, $J = 8.0 \text{ Hz}$, 4H, Ar-H), 7.02 (d, $J = 7.9 \text{ Hz}$, 4H, Ar-H), 6.98 (d, $J = 8.0 \text{ Hz}$, 4H, Ar-H), 6.95 (d, $J = 8.0 \text{ Hz}$, 4H, Ar-H), 6.76 (s, 2H, Ar-H), 5.25 (s, 2H, CHAr_2), 2.62 (dq, $J = 23.1, 7.6 \text{ Hz}$, 8H, CH_2CH_3), 2.22 (s, 3H, Ar- CH_3), 1.24 (t, $J = 7.6 \text{ Hz}$, 6H, CH_2CH_3), 1.21 (t, $J = 7.6 \text{ Hz}$, 6H, CH_2CH_3), 1.13 (s, 3H, Ar- $\text{C}(\text{CH}_3)=\text{N}$). ^{13}C NMR (151 MHz, CDCl_3) δ 169.43 (C=N), 156.33, 148.50, 146.10, 141.94, 141.67, 141.46, 140.19, 136.10, 132.53, 131.46, 129.79, 129.43, 128.52, 127.75, 127.51, 124.58, 121.50, 51.34 (CHAr_2), 28.51 (CH_2CH_3), 28.49 (CH_2CH_3), 21.46 (Ar- CH_3), 17.03 (Ar- $\text{C}(\text{CH}_3)=\text{N}$), 15.67 (CH_2CH_3), 15.63 (CH_2CH_3). MALDI-TOF-MS (m/z): calcd for $\text{C}_{48}\text{H}_{50}\text{N}_2$: 654.4000, Found, 654.4003, $[\text{M} + \text{H}]^+$.



L2 (1.01 g, 66%). ^1H NMR (600 MHz, CDCl_3) δ 8.59 (d, $J = 4.1$ Hz, 1H, Ar-*H*), 8.05 (d, $J = 7.8$ Hz, 1H, Ar-*H*), 7.70 (t, $J = 7.2$ Hz, 1H, Ar-*H*), 7.39–7.29 (m, 1H, Ar-*H*), 7.03 (d, $J = 7.9$ Hz, 4H, Ar-*H*), 6.94 (dt, $J = 11.9, 8.0$ Hz, 12H, Ar-*H*), 6.71 (s, 2H, Ar-*H*), 5.21 (s, 2H, CHAr_2), 2.65–2.46 (m, 8H, $\text{CH}_2\text{CH}_2\text{CH}_2\text{CH}_3$), 2.19 (s, 3H, Ar- CH_3), 1.68–1.48 (m, 8H, $\text{CH}_2\text{CH}_2\text{CH}_2\text{CH}_3$), 1.45–1.20 (m, 8H, $\text{CH}_2\text{CH}_2\text{CH}_2\text{CH}_3$), 1.08 (s, 3H, Ar- $\text{C}(\text{CH}_3)=\text{N}$), 0.92 (q, $J = 7.1$ Hz, 12H, $\text{CH}_2\text{CH}_2\text{CH}_2\text{CH}_3$). ^{13}C NMR (151 MHz, CDCl_3) δ 169.39 (C=N), 156.32, 148.49, 146.12, 141.41, 140.56, 140.32, 140.14, 136.03, 132.56, 131.40, 129.72, 129.35, 128.50, 128.30, 128.04, 124.53, 121.47, 51.35 (CHAr_2), 35.34 ($\text{CH}_2\text{CH}_2\text{CH}_2\text{CH}_3$), 35.27 ($\text{CH}_2\text{CH}_2\text{CH}_2\text{CH}_3$), 33.72 ($\text{CH}_2\text{CH}_2\text{CH}_2\text{CH}_3$), 33.70 ($\text{CH}_2\text{CH}_2\text{CH}_2\text{CH}_3$), 22.52 ($\text{CH}_2\text{CH}_2\text{CH}_2\text{CH}_3$), 22.41 ($\text{CH}_2\text{CH}_2\text{CH}_2\text{CH}_3$), 21.45 (Ar- CH_3), 16.99 (Ar- $\text{C}(\text{CH}_3)=\text{N}$), 14.09 ($\text{CH}_2\text{CH}_2\text{CH}_2\text{CH}_3$), 14.05 ($\text{CH}_2\text{CH}_2\text{CH}_2\text{CH}_3$). MALDI-TOF-MS (m/z): calcd for $\text{C}_{55}\text{H}_{66}\text{N}_2$: 766.5200, Found, 766.5245, $[\text{M} + \text{H}]^+$.

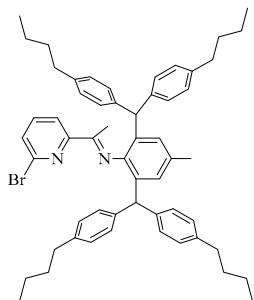


L3 (1.06 g, 72%). ^1H NMR (600 MHz, CDCl_3) δ 7.97 (d, $J = 7.6$ Hz, 1H, Ar-*H*), 7.55 (t, $J = 7.7$ Hz, 1H, Ar-*H*), 7.53–7.49 (m, 1H, Ar-*H*), 7.06 (d, $J = 8.0$ Hz, 4H, Ar-*H*), 7.02 (d, $J = 8.0$ Hz, 4H, Ar-*H*), 6.95 (d, $J = 8.0$ Hz, 4H, Ar-*H*), 6.91 (d, $J = 8.1$ Hz, 4H, Ar-*H*), 6.72 (s, 2H, Ar-*H*), 5.16 (s, 2H, CHAr_2), 2.66–2.54 (m, 8H, CH_2CH_3), 2.19 (s, 3H, Ar- CH_3), 1.26–1.19 (m, 12H, CH_2CH_3), 1.12 (s, 3H, Ar- $\text{C}(\text{CH}_3)=\text{N}$). ^{13}C NMR (151 MHz, CDCl_3) δ 168.54 (C=N), 157.40, 145.77, 142.06, 141.73, 141.17, 140.75, 140.04, 138.42, 132.44, 131.73, 129.74, 129.39, 128.95, 128.49, 127.82, 127.53, 120.12, 51.45 (CHAr_2), 28.52 (CH_2CH_3), 28.50 (CH_2CH_3), 21.44 (Ar- CH_3), 17.01 (Ar- $\text{C}(\text{CH}_3)=\text{N}$), 15.72 (CH_2CH_3), 15.62 (CH_2CH_3). APCI-MS (m/z): calcd for $\text{C}_{48}\text{H}_{49}\text{BrN}_2$: 735.3092, Found, 735.3110, $[\text{M} + \text{H}]^+$.



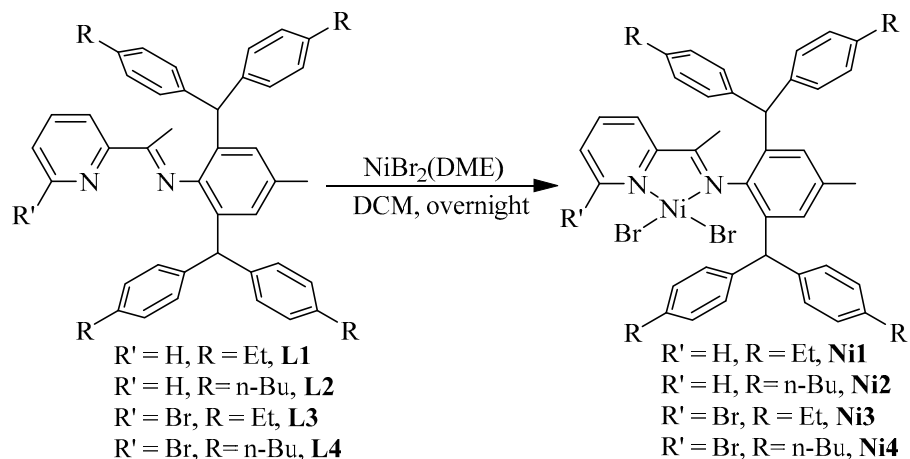
L4 (1.02 g, 60%). ^1H NMR (600 MHz, CDCl_3) δ 8.05 (dd, $J = 7.5, 0.9$ Hz, 1H, Ar-*H*), 7.60–7.50 (m, 2H, Ar-*H*), 7.10 (d, $J = 8.1$ Hz, 4H, Ar-*H*), 7.06 (d, $J = 8.0$ Hz, 4H, Ar-*H*), 7.01 (d, $J = 8.0$ Hz, 4H, Ar-*H*), 6.97 (d, $J = 7.9$ Hz, 4H, Ar-*H*), 6.78 (s, 2H, Ar-*H*), 5.23 (s, 2H, CHAr_2), 2.63 (dd, $J = 16.3, 8.8$ Hz, 8H, $\text{CH}_2\text{CH}_2\text{CH}_2\text{CH}_3$), 2.24 (s, 3H, Ar- CH_3), 1.70–1.58 (m, 8H, $\text{CH}_2\text{CH}_2\text{CH}_2\text{CH}_3$), 1.45–1.35 (m, 8H, $\text{CH}_2\text{CH}_2\text{CH}_2\text{CH}_3$), 1.14 (s, 3H, Ar- $\text{C}(\text{CH}_3)=\text{N}$), 0.99 (t, $J = 7.3$ Hz, 12H, $\text{CH}_2\text{CH}_2\text{CH}_2\text{CH}_3$). ^{13}C NMR (151 MHz, CDCl_3)

δ 168.64 (C=N), 157.42, 145.89, 141.19, 140.82, 140.74, 140.45, 140.06, 138.43, 132.57, 131.74, 129.76, 129.40, 129.00, 128.55, 128.49, 128.14, 120.12, 51.58 (CHAr₂), 35.39 (CH₂CH₂CH₂CH₃), 35.34 (CH₂CH₂CH₂CH₃), 33.79 (CH₂CH₂CH₂CH₃), 22.58 (CH₂CH₂CH₂CH₃), 22.43 (CH₂CH₂CH₂CH₃), 21.49 (Ar-CH₃), 16.99 (Ar-C(CH₃)=N), 14.16 (CH₂CH₂CH₂CH₃), 14.14 (CH₂CH₂CH₂CH₃). APCI-MS (*m/z*): calcd for C₅₆H₆₅BrN₂: 847.4344, Found, 847.4363, [M + H]⁺.

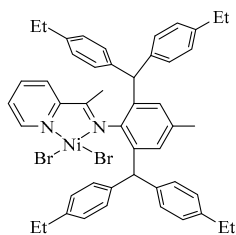


4.3. Procedure for the Synthesis of Nickel Complexes Ni1–Ni4

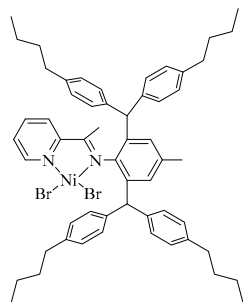
Complexes **Ni1–Ni4** were synthesized by the reaction of 1 equiv. of NiBr₂(DME) with the corresponding ligands in methylene chloride. The corresponding ligand (0.2 mmol) was added in 5 mL of methylene chloride in a Schlenk tube under a nitrogen atmosphere. NiBr₂(DME) (0.2 mmol, 62 mg) was added to the above solution. The resulting mixture was stirred at room temperature overnight. The solvent was evaporated under reduced pressure to afford a solid. The product was washed with 4 × 5 mL hexane and dried under vacuum. A single crystal could be obtained by diffusion from layering hexanes on to the CH₂Cl₂ solution at room temperature.



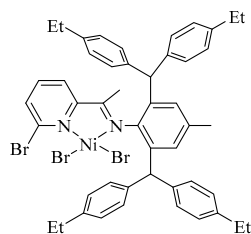
Ni1 (0.14 g, 80%), Elem. Anal. Calcd for C₄₈H₅₀Br₂N₂Ni: C, 66.01; H, 5.77; N, 3.21. Found: C, 66.21; H, 5.59; N, 3.11. MALDI-TOF-MS (*m/z*): calcd for C₄₈H₅₀BrN₂Ni: 791.2511, Found, 791.2515, [M – Br]⁺.



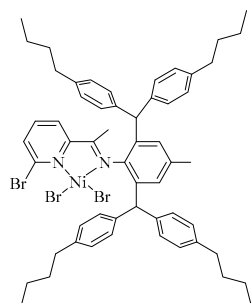
Ni2 (0.17 g, 85%). Elem. Anal. Calcd for $C_{56}H_{66}Br_2N_2Ni$: C, 68.24; H, 6.75; N, 2.84. Found: C, 68.35; H, 6.95; N, 3.05. MALDI-TOF-MS (m/z): calcd for $C_{56}H_{66}BrN_2Ni$: 903.3763, Found, 903.3737, $[M - Br]^+$.



Ni3 (0.15 g, 80%). Elem. Anal. Calcd for $C_{48}H_{49}Br_3N_2Ni$: C, 60.54; H, 5.19; N, 2.94. Found: C, 60.35; H, 5.27; N, 3.01. MALDI-TOF-MS (m/z): calcd for $C_{48}H_{49}Br_2N_2Ni$: 869.1616, Found, 869.1609, $[M - Br]^+$.



Ni4 (0.16 g, 75%). Elem. Anal. Calcd for $C_{56}H_{65}Br_3N_2Ni$: C, 63.18; H, 6.15; N, 2.63. Found: C, 63.35; H, 6.28; N, 2.72. MALDI-TOF-MS (m/z): calcd for $C_{56}H_{65}Br_2N_2Ni$: 981.2868, Found, 981.2879, $[M - Br]^+$.



4.4. A General Procedure for the Ethylene Oligomerization Using Ni Complexes

In a typical experiment, a pressure glass reactor with a 350 mL thick wall, connected with a high-pressure gas line, was first dried at 90 °C under vacuum for at least 1 h. The reactor was then adjusted to the desired oligomerization temperature. Then, 20 mL of toluene and the desired amount Et_2AlCl was added to the reactor under N_2 atmosphere, and the desired amount of catalyst in 1 mL of CH_2Cl_2 was injected into the oligomerization system via syringe. With rapid stirring, the reactor was pressurized and maintained at 6 atm of ethylene. After 60 min, the pressure reactor was vented and the ethylene oligomers were obtained under vacuum.

Supplementary Materials: The following are available online at <https://www.mdpi.com/article/10.3390/polym14153049/s1>. NMR, GPC and GC-MS curves of oligomers samples, single crystal data of **Ni1**.

Author Contributions: Conceptualization, S.D.; methodology, J.C. and Z.Y.; validation, S.D.; formal analysis, J.C.; investigation, J.C. and Z.Y.; resources, J.C.; data curation, S.D.; writing—original draft preparation, S.D.; writing—review and editing, S.D., Z.Y. and Z.L.; supervision, S.D.; project administration, S.D.; funding acquisition, S.D. All authors have read and agreed to the published version of the manuscript.

Funding: This research was funded by Natural Science Foundation of Anhui Province (2108085Y06) and Anhui Provincial Key Laboratory Open Project Foundation (LCECSC-01).

Data Availability Statement: All the data can be obtained in the supplementary materials or by contacting the corresponding author.

Acknowledgments: This work was supported by Natural Science Foundation of Anhui Province (2108085Y06), Anhui Provincial Key Laboratory Open Project Foundation (LCECSC-01).

Conflicts of Interest: The authors declare no conflict of interest.

References

1. Erhard, G. *Designing with Plastics*; Hanser Gardner Publications: Cincinnati, OH, USA, 2006.
2. Vasile, C.; Marcel, D. *Handbook of Polyolefins*; CRC Press: New York, NY, USA, 2000.
3. Chung, T.C. *Functionalization of Polyolefins*; Academic Press: London, UK, 2002.
4. Gibson, V.C.; Tomov, A. Functionalised polyolefin synthesis using [P,O]Ni catalysts. *Chem. Commun.* **2001**, *19*, 1964–1965. [[CrossRef](#)] [[PubMed](#)]
5. Hong, S.C.; Jia, S.; Teodorescu, M.; Kowalewski, T.; Matyjaszewski, K.; Gottfried, A.C.; Brookhart, M. Polyolefin graft copolymers via living polymerization techniques: Preparation of poly(n-butyl acrylate)-graft-polyethylene through the combination of Pd-mediated living olefin polymerization and atom transfer radical polymerization. *J. Polym. Sci. Part A Polym. Chem.* **2002**, *40*, 2736–2749. [[CrossRef](#)]
6. Gottfried, A.C.; Brookhart, M. Living and Block Copolymerization of Ethylene and α -Olefins Using Palladium(II)- α -Diimine Catalysts. *Macromolecules* **2003**, *36*, 3085–3100. [[CrossRef](#)]
7. Makio, H.; Fujita, T. Synthesis of Chain-End Functionalized Polyolefins with a Bis(phenoxy imine)Titanium Catalyst. *Macromol. Rapid Commun.* **2007**, *28*, 698–703. [[CrossRef](#)]
8. Amin, S.B.; Marks, T.J. Versatile Pathways for In Situ Polyolefin Functionalization with Heteroatoms: Catalytic Chain Transfer. *Angew. Chem. Int. Ed.* **2008**, *47*, 2006–2025. [[CrossRef](#)] [[PubMed](#)]
9. Valente, A.; Mortreux, A.; Visseaux, M.; Zinck, P. Coordinative Chain Transfer Polymerization. *Chem. Rev.* **2013**, *113*, 3836–3857. [[CrossRef](#)] [[PubMed](#)]
10. Fu, P.-F.; Marks, T.J. Silanes as Chain Transfer Agents in Metallocene-Mediated Olefin Polymerization. Facile in Situ Catalytic Synthesis of Silyl-Terminated Polyolefins. *J. Am. Chem. Soc.* **1995**, *117*, 10747–10748. [[CrossRef](#)]
11. Xu, G.; Chung, T.C. Borane Chain Transfer Agent in Metallocene-Mediated Olefin Polymerization. Synthesis of Borane-Terminated Polyethylene and Diblock Copolymers Containing Polyethylene and Polar Polymer. *J. Am. Chem. Soc.* **1999**, *121*, 6763–6764. [[CrossRef](#)]
12. Bazan, G.C.; Rogers, J.S.; Fang, C.C. Catalytic Insertion of Ethylene into Al-C Bonds with Pentamethylcyclopentadienyl-Chromium(III) Complexes. *Organometallics* **2001**, *20*, 2059–2064. [[CrossRef](#)]
13. German, I.; Kelhifi, W.; Norsic, S.; Boisson, C.; D’Agosto, F. Telechelic Polyethylene from Catalyzed Chain-Growth Polymerization. *Angew. Chem. Int. Ed.* **2013**, *52*, 3438–3441. [[CrossRef](#)] [[PubMed](#)]
14. Kawaoka, A.M.; Marks, T.J. Organolanthanide-Catalyzed Synthesis of Phosphine-Terminated Polyethylenes. *J. Am. Chem. Soc.* **2004**, *126*, 12764–12765. [[CrossRef](#)] [[PubMed](#)]
15. Amin, S.B.; Marks, T.J. Organolanthanide-Catalyzed Synthesis of Amine-Capped Polyethylenes. *J. Am. Chem. Soc.* **2007**, *129*, 10102–10103. [[CrossRef](#)] [[PubMed](#)]
16. Ringelberg, S.N.; Meetsma, A.; Hessen, B.; Teuben, J.H. Thiophene C–H Activation as a Chain-Transfer Mechanism in Ethylene Polymerization: Catalytic Formation of Thienyl-Capped Polyethylene. *J. Am. Chem. Soc.* **1999**, *121*, 6082–6083. [[CrossRef](#)]
17. Wang, X.; Nozaki, K. Selective Chain-End Functionalization of Polar Polyethylenes: Orthogonal Reactivity of Carbene and Polar Vinyl Monomers in Their Copolymerization with Ethylene. *J. Am. Chem. Soc.* **2018**, *140*, 15635–15640. [[CrossRef](#)] [[PubMed](#)]
18. Wiedemann, T.; Voit, G.; Tchernook, A.; Roesle, P.; Göttker-Schnetmann, I.; Mecking, S. Monofunctional hyperbranched ethylene oligomers. *J. Am. Chem. Soc.* **2014**, *136*, 2078–2085. [[CrossRef](#)] [[PubMed](#)]
19. Mecking, S.; Schütte, M. Neutral nickel(II) catalysts: From hyperbranched oligomers to nanocrystal-based materials. *Acc. Chem. Res.* **2020**, *53*, 2738–2752. [[CrossRef](#)] [[PubMed](#)]
20. Stephenson, C.J.; McInnis, J.P.; Chen, C.; Weberski, M.P.; Motta, A.; Delferro, M.; Marks, T.J. Ni(II) phenoxyiminato olefin polymerization catalysis: Striking coordinative modulation of hyperbranched polymer microstructure and stability by a proximate sulfonyl group. *ACS Catal.* **2014**, *4*, 999–1003. [[CrossRef](#)]
21. Falivene, L.; Wiedemann, T.; Göttker-Schnetmann, I.; Caporaso, L.; Cavallo, L.; Mecking, S. Control of chain walking by weak neighboring group interactions in unsymmetrical catalysts. *J. Am. Chem. Soc.* **2018**, *140*, 1305–1312. [[CrossRef](#)]

22. Xiang, P.; Ye, Z.; Subramanian, R. Synthesis and characterization of low- and medium-molecular-weight hyperbranched polyethylenes by chain walking ethylene polymerization with Pd-diimine catalysts. *Polymer* **2011**, *52*, 5027–5039. [[CrossRef](#)]
23. Meduri, A.; Montini, T.; Ragaini, F.; Fornasiero, P.; Zangrando, E.; Milani, B. Palladium-catalyzed ethylene/methyl acrylate co-oligomerization: Effect of a new nonsymmetric α -diimine. *ChemCatChem* **2013**, *5*, 1170–1183. [[CrossRef](#)]
24. Guo, L.; Liu, W.; Li, K.; Sun, M.; Sun, W.; Zhao, L.; Jiang, G.; Peng, H.; Liu, Z.; Dai, S. Synthesis of functional and hyperbranched ethylene oligomers using unsymmetrical α -diimine palladium catalysts. *Eur. Polym. J.* **2019**, *115*, 185–192. [[CrossRef](#)]
25. Cruz, T.F.C.; Figueira, C.A.; Veiros, L.F.; Gomes, P.T. Benzylnickel(II) complexes of 2-iminopyrrolyl chelating ligands: Synthesis, structure, and catalytic oligo-/polymerization of ethylene to hyperbranched polyethylene. *Organometallics* **2021**, *40*, 2594–2609. [[CrossRef](#)]
26. Wang, C.; Zhang, Y.; Mu, H.; Jian, Z. Systematic studies on dibenzhydryl and pentiptycenylyl substituted pyridine-imine nickel(II) mediated ethylene polymerization. *Dalton Trans.* **2020**, *49*, 4824–4833. [[CrossRef](#)] [[PubMed](#)]
27. Guo, L.; Li, S.; Ji, M.; Sun, W.; Liu, W.; Li, G.; Zhang, J.; Liu, Z.; Dai, S. Monoligated vs bisligated effect in iminopyridyl nickel catalyzed ethylene polymerization. *Organometallics* **2019**, *38*, 2800–2806. [[CrossRef](#)]
28. Chen, X.; Gao, J.; Liao, H.; Gao, H.; Wu, Q. Synthesis, characterization, and catalytic ethylene oligomerization of pyridine-imine palladium complexes. *Chin. J. Polym. Sci.* **2018**, *36*, 176–184. [[CrossRef](#)]
29. Li, S.; Lu, Z.; Fan, W.; Dai, S. Efficient incorporation of a polar comonomer for direct synthesis of hyperbranched polar functional ethylene oligomers. *New J. Chem.* **2021**, *45*, 4024–4031. [[CrossRef](#)]
30. Yan, Z.; Li, S.; Dai, S. Synthesis and characterization of hyperbranched polar functionalized olefin oligomers. *Chin. J. Synth. Chem.* **2021**, *29*, 1033–1044.
31. Saki, Z.; D'Auria, I.; Dall'Anese, A.; Milani, B.; Pellicchia, C. Copolymerization of ethylene and methyl acrylate by pyridylimino Ni(II) catalysts affording hyperbranched poly(ethylene-co-methyl acrylate)s with tunable structures of the ester groups. *Macromolecules* **2020**, *53*, 9294–9305. [[CrossRef](#)]
32. D'Auria, I.; Milione, S.; Caruso, T.; Balducci, G.; Pellicchia, C. Synthesis of hyperbranched low molecular weight polyethylene oils by an iminopyridine nickel(II) catalyst. *Polym. Chem.* **2017**, *8*, 6443–6454. [[CrossRef](#)]
33. Fan, H.; Chang, G.; Bi, H.; Gui, X.; Wang, H.; Xu, G.; Dai, S. Facile synthesis of hyperbranched ethylene oligomers and ethylene-methyl acrylate co-oligomers with different microscopic chain architectures. *ACS Polym. Au* **2022**, *2*, 88–96. [[CrossRef](#)]
34. Yan, Z.; Bi, H.; Ding, B.; Wang, H.; Xu, G.; Dai, S. A rigid-flexible double-layer steric strategy for ethylene (co)oligomerization with pyridine-imine Ni(II) and Pd(II) complexes. *New J. Chem.* **2022**, *46*, 8669–8678. [[CrossRef](#)]
35. Fan, H.; Xu, G.; Wang, H.; Dai, S. Direct synthesis of hyperbranched ethylene oligomers and ethylene-MA co-oligomers using iminopyridyl systems with weak neighboring group interactions. *J. Polym. Sci.* **2022**, *60*, 1944–1953. [[CrossRef](#)]
36. Cotts, P.M.; Guan, Z.; McCord, E.; McLain, S. Novel Branching Topology in Polyethylenes As Revealed by Light Scattering and ^{13}C NMR. *Macromolecules* **2000**, *33*, 6945–6952. [[CrossRef](#)]
37. Randall, J.C. A review of high-resolution liquid carbon-13 nuclear magnetic resonance characterizations of ethylene-based polymer. *J. Macromol. Sci. Part C Polym. Rev.* **1989**, *29*, 201–317. [[CrossRef](#)]
38. Galland, G.B.; de Souza, R.F.; Mauler, R.S.; Nunes, F.F. ^{13}C NMR Determination of the Composition of Linear Low-Density Polyethylene Obtained with $[\eta^3\text{-Methallyl-nickel-diimine}]\text{PF}_6$ Complex. *Macromolecules* **1999**, *32*, 1620–1625. [[CrossRef](#)]